Chapter 4 Enhancement of Electrical properties of $BiFeO_3$ multiferroic material by co-doping

4.1 Introduction

Multiferroics materials which simultaneously show a couple of primary ferroics or non–ferroics order parameter at the same substance are constantly under intense investigation in last closing several years in view of its ability applications such as high sensitivity ac magnetic field sensor, data-storage media, in typical Spintronics device e.g. MTJ (Magnetic tunnel junction) to manufacture extra logic states and many more [96]**.** In ME multiferroics, electric and magnetic orders co-exist and mutual controllability between them is known as ME coupling**]** [97].n last several years, there are numerous multiferroics materials discovered among them BFO is most promising multiferroic material having both ferroelectric transition temperature (T_C =1100 K) and antiferromagnetic (T_N = 650 K) have large values[30]. The crystal structure of BFO is rhombohedral distorted perovskite structural belonging to space group R3c [98]. BFO has been shown to large spontaneous polarization of order 10-100μc/cm^2 due to the polar displacement of cations and anions relative to each other pointing along one of the eight pseudo-cubic [111] axes [99]**.** But, single phase polycrystalline BFO shows low resistivity, large leakage current, and weak ME coupling make it limited for device applications. In order to reduce this lacking of single phase BFO, extensive research in the pastfew years has already used doping and co-doping methods and to enhance and stabilize the multiferroic properties. B. et al. improved the multiferroics properties of BFO by subsisting La and Mn co-doped on BFO nanofibers [100]. In present work, we have substituted Al on the Mn site of $Bi_{0.5}La_{0.5}Fe_{0.5}Mn_{0.5}O_3$ and improve the ferroelectricity property of BFO**.**

4.2 Experimental procedures:

$Bi_{0.5}La_{0.5}Fe_{0.5}Mn_{0.5-x}Al_xO_3$ (with x = 0.0 and 0.1) are prepared by the solid-state reaction method. Highly pure oxides Bi_2O_3, Fe_2O_3, La_2O_3, TiO_2, MnO_2 and Al_2O_3 in a stoichiometric ratio and mixed in an agate mortar for 2h and calcined in an aluminum crucible at 850 °C for 24 h. After calcination, obtained powders were ground and sintered at 950 °C for 12 h. The obtained samples were characterized by X-ray diffraction (Model: Miniflex-II, Rigaku, Japan) with Cu Kα radiation (λ = 1.5406 Å). The room temperature Raman spectra were performed by Renishaw micro-Raman spectroscope in the range of 200 cm^{-1} to 800 cm^{-1} using 514.5 nm Ar^+ laser as excitation source. The measurement of dielectric constant (ε') and dissipation factor (tanδ) were characterized by Agilent E4980A Precision LCR meter.

4.3 RESULTS AND DISCUSSION

4.3.1 X-ray diffraction analysis

The room temperature X-ray diffraction patterns of $Bi_{0.5}La_{0.5}Fe_{0.5}Mn_{0.5-x}Al_xO_3$ (with x = 0.0 and 0.1) are shown in Figure.(4.1). It can be seen inFigure 1; there is no extra peaks of impurity phases (like $Bi_2Fe_4O_9$ and $Bi_{25}FeO_4$) are present in $Bi_{0.5}La_{0.5}Fe_{0.5}Mn_{0.5}O_3$and $Bi_{0.5}La_{0.5}Fe_{0.5}Mn_{0.40}Al_{0.1}O_3$ samples. This outcome suggests that the replacement of 20% of Mn in $Bi_{0.5}La_{0.5}Fe_{0.5}Mn_{0.5}O_3$ by Al does not change the structure and system remains orthorhombic symmetry belonging to the space group *Pnma*. We have also reported orthorhombic structural with space group Pnma in $Bi_{0.5}La_{0.5}Fe_{0.5}Mn_{0.45}Ti_{0.05}O_3$ in our previous work [101]. Rietveld refinements of the XRD pattern shown in Figure 1 have been refined by the full proof software

package. The calculated, observed and difference profile confirms that the systemis of a single phase.

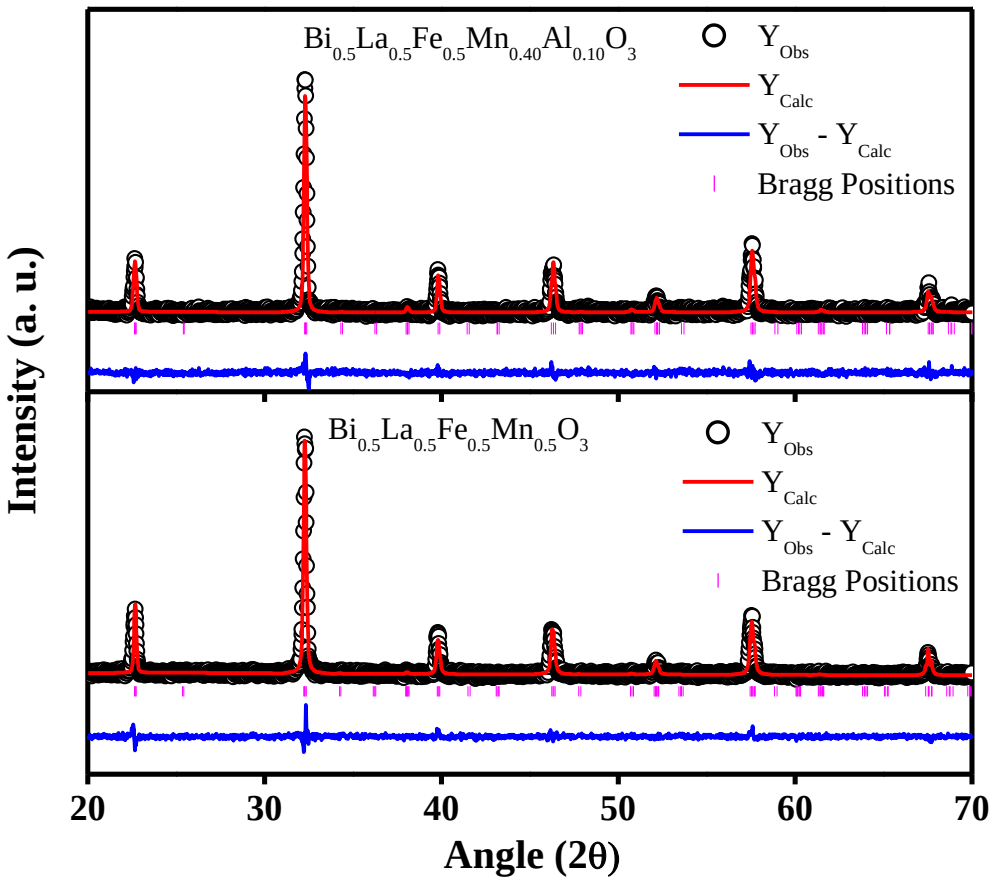

Figure 4.1 Rietveld refinement profiles of X-ray diffraction patterns of $Bi_{0.5}La_{0.5}Fe_{0.5}Mn_{0.5}O_3$ and $Bi_{0.5}La_{0.5}Fe_{0.5}Mn_{0.40}Al_{0.1}O_3$ samples.

4.3.2 Raman Spectroscopy:

To examine the atomic displacements, defects in the host and structural change due to doping of Al on La and Mn co-doped BFO, we have carried out room temperature Raman spectra in the range of 200 cm^{-1} to 1000 cm^{-1} as show 36n in Figure 4.2. Theoretical group analysis predicted

18 optical phonon modes ($\Gamma_{Raman,R3c}$=4A_1 + 5A_2+9E) in which 13(4A_1+9E) modes are Raman and IR-active for rhombohedral distorted perovskite BFO[36]. Singh et al. also reported 10 Raman active modes out of those 13 possible Raman modes for La and Mn co-doped BFO [9]. In this work, we observed two weak Raman modes A_1-3 (at ~220 cm^{-1}) , E-2 (at ~255 cm^{-1}) and three strong modes E-5(~476.9), E-6 (~535) and E-7(599.6 cm^{-1}) in both the samples. It is because of the fact that Raman modes depends on the number of atoms and the size of the unit cell and usually, Raman modes are expected to decrease with the increase of the number of the atoms in the unit cell [101, 102]. It clearly indicates that there is no crystal structure transition due to the Al substituted $Bi_{0.5}La_{0.5}Fe_{0.5}Mn_{0.5}O_3$.

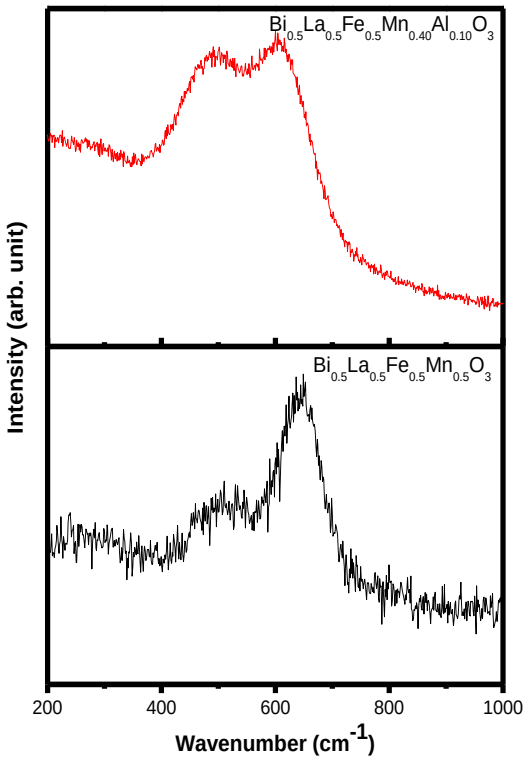

Figure 4.2. Room-temperature micro-Raman spectra of $Bi_{0.5}La_{0.5}Fe_{0.5}Mn_{0.5}O_3$ and $Bi_{0.5}La_{0.5}Fe_{0.5}Mn_{0.40}Al_{0.1}O_3$ samples.

4.3.3 Dielectric Property:

Figure 4.3 shows the temperature variation of the real part of the dielectric constant (ε') and dissipation factor (tanδ) at different frequencies (1kHz-2MHz) for $Bi_{0.5}La_{0.5}Fe_{0.5}Mn_{0.5}O_3$ and $Bi_{0.5}La_{0.5}Fe_{0.5}Mn_{0.40}Al_{0.10}O_3$. It can be seen from Figure 4.3 that above 200K ε' increases sharply for both samples and shows a giant dielectric constant. It has been observed that the replacement of 20% Mn by Al enhances ε' ~8.5×10^3 for $Bi_{0.5}La_{0.5}Fe_{0.5}Mn_{0.5}O_3$ to ~1×10^4 for $Bi_{0.5}La_{0.5}Fe_{0.5}Mn_{0.40}Al_{0.10}O_3$ at room temperature. This increase of dielectric constant ε' by substitution of Al at Mn site can be understood by hopping mechanism. At low frequency, Al doped $Bi_{0.5}La_{0.5}Fe_{0.5}Mn_{0.5}O_3$ increase defect near the grain boundary and increase interwell hopping mechanism which results in increment of the dielectric constant. At higher frequency ε'increses due to the dominance of intra-well hopping [103]. As we increase the Along with Maxwell–Wanger relaxation, ferroelectric relaxor behavior might also be responsible for the large dielectric constant as the loss peak shift towards the higher temperature with increasing frequency [104].

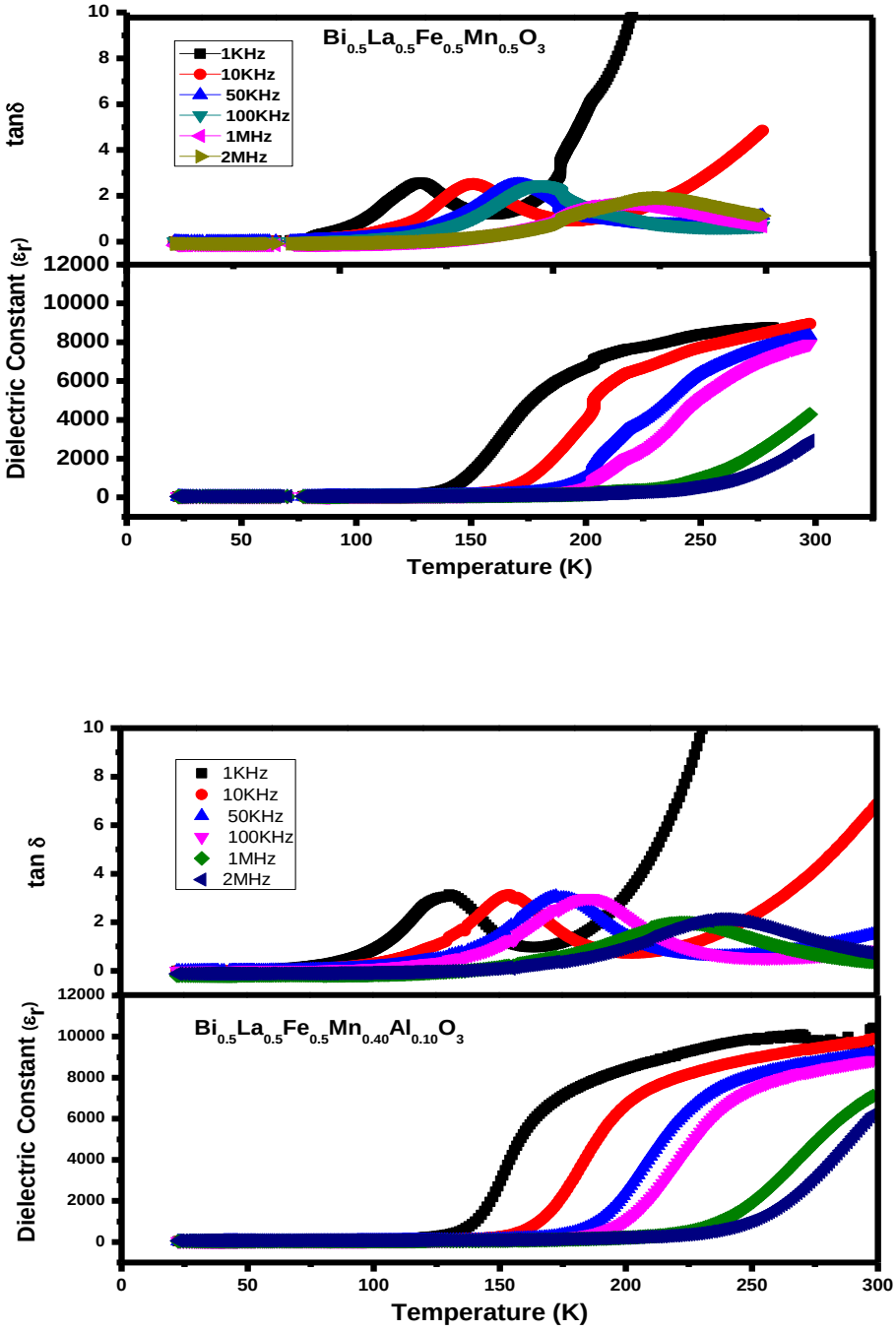

Figure 4.3. Variation of ε' and tan(δ) values with respect to temperature at 1KHz,10KHz,50KHz,100KHz,1MHz and 2MHz for (a)$Bi_{0.5}La_{0.5}Fe_{0.5}Mn_{0.5}O_3$ and (b) $Bi_{0.5}La_{0.5}Fe_{0.5}Mn_{0.40}Al_{0.1}O_3$.

4.4 Conclusions

In this chapter, we successfully prepared $Bi_{0.5}La_{0.5}Fe_{0.5}Mn_{0.5-x}Al_xO_3$ (where x=0 and 0.1) by solid state route. The XRD with Rietveld refinement shows that $Bi_{0.5}La_{0.5}Fe_{0.5}Mn_{0.5}O_3$and $Bi_{0.5}La_{0.5}Fe_{0.5}Mn_{0.40}Al_{0.10}O_3$ sample is formed in a single phase without the presence of any impurity phase Room temperature Raman study also reveals that is no structural transition have been observed with Al-doped $Bi_{0.5}La_{0.5}Fe_{0.5}Mn_{0.5}O_3$.Dielectric measurement shows that substitution of Al at Mn site enhanced the dielectric properties which might be due to Maxwell – Wagner effect.